

Chiral symmetry breaking, color superconductivity and quark matter phase diagram: a variational approach

Hiranmaya Mishra ^{*} and Jitendra C. Parikh [†]

Theory Division, Physical Research Laboratory, Navrangpura, Ahmedabad 380 009, India

We discuss in this note simultaneous existence of chiral symmetry breaking and color superconductivity at finite temperature and density in a Nambu-Jona-Lasinio type model. The methodology involves an explicit construction of a variational ground state and minimisation of the thermodynamic potential. There exists solutions to the gap equations at finite densities with both quark antiquark as well as diquark condensates for the “ground” state. However, such a phase is thermodynamically unstable with the pressure being negative in this region. We also compute the equation of state, and obtain the structure of the phase diagram in the model.

PACS number(s): 12.38.Gc

I. INTRODUCTION

The structure of vacuum in Quantum Chromodynamics (QCD) is one of the most interesting questions in strong interaction physics [1]. The evidence for quark and gluon condensates in vacuum is a reflection of its complex nature [2], whereas chiral symmetry breaking is an essential feature in the description of the low mass hadron properties. Due to the nonperturbative nature of QCD in this regime different effective models have been used to understand the nature of chiral symmetry breaking. These have been constructed, for the most part, in the framework of a Nambu-Jona-Lasinio (NJL) model with a four fermion interaction. There also have been attempts to generalise this in the case of Coulomb gauge QCD with an effective propagator simulating the effects of confining potentials [3–9]. Studies at finite temperatures using imaginary time formulation of finite temperature field theory [11] have also been carried out.

Recently there has been a lot of interest in strongly interacting matter at high densities. In particular, a color superconducting phase for it involving diquark condensates has been considered with a gap of about 100 MeV. The studies have been done with an effective four fermion interaction between quarks [12], direct instanton approach [13] or a perturbative QCD calculation at finite density [14]. There has also been a study of this phase in NJL model [15]. In the NJL model however, the aspect of chiral symmetry breaking in presence of diquark condensates has not been considered. Such a question has been considered in Ref. [16] in an instanton induced four fermion interaction model within a mean field approximation. In this note, we use a different method to study the problem. We consider a variational approach with an explicit assumption for the ground state having both quark antiquark and diquark condensates. The actual calculations are carried out for the NJL model such that the minimisation of the free energy density determines which condensate will exist at what density.

We organise this paper as follows. In section **II** we construct the ground state as a vacuum realignment with quark antiquark as well as diquark condensates. The finite temperature and density effects are included within the framework of thermofield dynamics [17] through a thermal Bogoliubov transformation involving doubling of the Hilbert space. In section **III** we shall consider an effective model as is considered for chiral symmetry breaking in Coulomb gauge QCD [3–5]. To solve the gap equation exactly we shall further take a four fermion point interaction limit of the same similar to NJL model. In section **IV** we solve the gap equations for the mass and the superconducting gap, determine the phase diagram and discuss the results. Finally, we give a summary in section **V**.

II. AN ANSATZ FOR THE GROUND STATE

As noted earlier we shall include here the effects of both chiral symmetry breaking as well as diquark pairing. For the consideration of chiral symmetry breaking, we shall take the perturbative vacuum state with chiral symmetry as

^{*}email address hm@prl.ernet.in

[†]email address parikh@prl.ernet.in

$|0\rangle$. In this basis we shall take the quarks as massless. We shall then assume a specific vacuum realignment which breaks chiral symmetry because of interaction.

We have seen earlier that chiral symmetry breaking takes place with the formation of quark antiquark condensates in perturbative vacuum [9,10,18–22]. We consider the quark field operator expansion in momentum space given as [9,10,18,19]

$$\begin{aligned}\psi(\mathbf{x}) &\equiv \frac{1}{(2\pi)^{3/2}} \int \tilde{\psi}(\mathbf{k}) e^{i\mathbf{k}\cdot\mathbf{x}} d\mathbf{k} \\ &= \frac{1}{(2\pi)^{3/2}} \int [U_0(\mathbf{k}) q_I^0(\mathbf{k}) + V_0(-\mathbf{k}) \tilde{q}_I^0(-\mathbf{k})] e^{i\mathbf{k}\cdot\mathbf{x}} d\mathbf{k},\end{aligned}\quad (1)$$

where [20,21]

$$\begin{aligned}U_0(\mathbf{k}) &= \frac{1}{\sqrt{2}} \begin{pmatrix} 1 \\ \sigma \cdot \hat{k} \end{pmatrix}, \\ V_0(-\mathbf{k}) &= \frac{1}{\sqrt{2}} \begin{pmatrix} -\sigma \cdot \hat{k} \\ 1 \end{pmatrix}.\end{aligned}\quad (2)$$

The subscript I and the superscript 0 indicate that the operators q_I^0 and \tilde{q}_I^0 are two component ones which annihilate or create quanta acting upon the perturbative or the chiral vacuum.

We now consider vacuum destabilisation leading to chiral symmetry breaking [9,10,18,19] described by,

$$|vac\rangle = \mathcal{U}_Q |0\rangle, \quad (3)$$

where

$$\mathcal{U}_Q = \exp \left(\int q_I^0(\mathbf{k})^\dagger (\boldsymbol{\sigma} \cdot \mathbf{k}) h(\mathbf{k}) \tilde{q}_I^0(\mathbf{k}) d\mathbf{k} - h.c. \right). \quad (4)$$

In the above, we have suppressed the flavor and color indices on the two component quark and antiquark operators. Further $h(\mathbf{k})$ is a real function of $|\mathbf{k}|$ which describes vacuum realignment for quarks of a given flavor. We consider here two flavors and take the condensate function $h(\mathbf{k})$ to be the same for u and d quarks. Clearly, a nontrivial $h(\mathbf{k})$ shall break chiral $SU(2)_L \times SU(2)_R$ symmetry to the custodial symmetry $SU(2)_V$ for the light quark doublet [19,22]. In what follows we shall exploit this result.

Having defined the state as in Eq.(3) for chiral symmetry breaking, we shall next define the state involving diquarks. We note that as per BCS result such a state will be dynamically favored if there is an attractive interaction between the quarks [23]. Such an interaction exists in QCD in the qq color antitriplet, Lorentz scalar and isospin singlet channel. In the flavor antisymmetric channel the interaction can be scalar, pseudoscalar or vector whereas in flavor symmetric channel only the axial vector channel is attractive. In the present work, we shall consider the ansatz state involving diquarks as

$$|\Omega\rangle = U_d |vac\rangle = \exp(B_d^\dagger - B_d) |vac\rangle, \quad (5)$$

where

$$B_d^\dagger = \frac{1}{2} \int \left[q_r^{ia}(\mathbf{k})^\dagger f(\mathbf{k}) q_{-r}^{jb}(-\mathbf{k})^\dagger \epsilon_{ij} \epsilon_{3ab} + \tilde{q}_r^{ia}(\mathbf{k}) f_1(\mathbf{k}) \tilde{q}_{-r}^{jb}(-\mathbf{k}) \epsilon_{ij} \epsilon_{3ab} \right] d\mathbf{k}. \quad (6)$$

In the above, i, j are flavor indices, a, b are the color indices and $r (= \pm 1/2)$ is the spin index. As noted earlier we shall consider systems with two flavors and three colors. We have also introduced here two trial functions $f(\mathbf{k})$ and $f_1(\mathbf{k})$ respectively for the diquark and diantiquark channel. As may be noted the state constructed in eq.(5) is spin singlet and is antisymmetric in color and flavor. The corresponding Bogoliubov transformation for the operators is given by

$$\begin{pmatrix} q_{Ir}^{ia}(\mathbf{k}) \\ q_{I-r}^{kc}(-\mathbf{k})^\dagger \end{pmatrix} = \begin{pmatrix} \cos f(\mathbf{k}) & -r \frac{f(\mathbf{k})}{|f(\mathbf{k})|} \epsilon_{ik} \epsilon_{3ac} \sin f(\mathbf{k}) \\ r \frac{f^*(\mathbf{k})}{|f(\mathbf{k})|} \epsilon_{ki} \epsilon_{3ca} \sin f(\mathbf{k}) & \cos f(\mathbf{k}) \end{pmatrix} \begin{pmatrix} q_{Ir}^{ia}(\mathbf{k}) \\ \tilde{q}_{I-r}^{kc}(-\mathbf{k}) \end{pmatrix}. \quad (7)$$

In a similar manner one can write down the Bogoliubov transformation for the antiquark operators corresponding to $|\Omega\rangle$ basis.

Finally, to include the effect of temperature and density we obtain the state at finite temperature and density $|\Omega(\beta, \mu)\rangle$ by a thermal Bogoliubov transformation over the state $|\Omega\rangle$ using thermofield dynamics (TFD) as described in ref.s [17,24,25]. We have,

$$|\Omega(\beta, \mu)\rangle = \mathcal{U}_{\beta, \mu} |\Omega\rangle \quad (8)$$

where $\mathcal{U}_{\beta, \mu}$ is

$$\mathcal{U}_{\beta, \mu} = e^{\mathcal{B}^\dagger(\beta, \mu) - \mathcal{B}(\beta, \mu)}, \quad (9)$$

with,

$$\mathcal{B}^\dagger(\beta, \mu) = \int d^3\mathbf{k} \left[q_I'(\mathbf{k})^\dagger \theta_-(\mathbf{k}, \beta, \mu) \underline{q}_I'(\mathbf{k})^\dagger + \tilde{q}_I'(\mathbf{k}) \theta_+(\mathbf{k}, \beta, \mu) \underline{\tilde{q}}_I'(\mathbf{k}) \right] d\mathbf{k}. \quad (10)$$

In Eq.(10) the ansatz functions $\theta_\pm(\mathbf{k}, \beta, \mu)$ will be related to quark and antiquark distributions and the underlined operators are the operators in the extended Hilbert space associated with thermal doubling in TFD method. Thus the ansatz functions at finite temperature and density given in Eq.(8) involves five functions - $h(\mathbf{k})$, for the quark anti quark condensates, $f(\mathbf{k})$ and $f_1(\mathbf{k})$ describing respectively the diquark and diantiquark condensates and $\theta_\pm(\mathbf{k}, \beta, \mu)$ to include the temperature and density effects. All these functions are to be obtained by minimising the thermodynamic potential. This will involve an assumption about the effective hamiltonian. We shall carry out this minimisation in the next section.

III. ESTIMATION OF THE PRESSURE AND THE MODEL

Since the low and medium energy behaviour of QCD is not well understood one has to make assumptions about the effective interaction between the quarks. To consider chiral symmetry breaking in the Coulomb gauge pairing model [4–6] one had the effective action

$$\mathcal{S}_{eff} = \int d^4x \bar{\psi}(x) (i\gamma^\mu \partial_\mu) \psi(x) + \frac{1}{2} \int d^4x \int d^4y g^2 (x-y) J_\mu^a D_{ab}^{\mu\nu}(x-y) J_\nu^b(y), \quad (11)$$

where,

$$J_\mu^a(x) = \bar{\psi}^k(x) \gamma_\mu \left(\frac{\lambda^a}{2} \right) \psi^k(x).$$

A sum over color indices a and b is implied, g is the strong coupling constant and, $D_{ab}^{\mu\nu}(x-y)$ is the full gluon propagator. This effective action may be thought of as resulting from integrating out the gluonic degrees of freedom from the full QCD Lagrangian keeping only the bilinear terms of the quark currents. While dealing with the gluon sector, to make things computable, one uses different approximations for the full propagator which is written down in Coulomb gauge [4–6,9,10]. The most obvious one is to neglect transeverse gluons completely maintaining only the instantaneous Coulomb interactions. This was done in Ref. [4,5] for chiral symmetry breaking. Another possiblity is to neglect retardation effects for the transverse gluons and have e.g. $D^{ij}(p) = D^{ij}(\mathbf{p}, p_0)$ - the so called Breit interaction. In such instantaneous approximations one can interpret the product of the coupling constant and the gluon propagator as the Fourier tranform of the effective quark antiquark potential. Different effective potentials such as confining, Richardson, and a screened potential for the transverse part have been considered for chiral symmetry breaking in Coulomb gauge pairing model [4–6].

To deal with the case of finite temperature and density one might take one loop resummed perturbative QCD results at finite temperature and densities [14,27] for the propagator. However, we shall here assume a point like interaction approximation. The reason we shall choose this is its simplicity regarding its solvability. Further we can compare the results with those of NJL model calculations [15]. The delta function interaction produces short distance singularities and so to regulate the integrals we shall restrict the phase space inside the sphere $|\mathbf{p}| < \Lambda$. Thus the effective Hamiltonian we shall be considering is given by

$$\mathcal{H} = \psi^\dagger (-i\boldsymbol{\alpha} \cdot \boldsymbol{\nabla}) \psi + \frac{g^2}{2} J_\mu^a J^{\mu a}. \quad (12)$$

We next write down the expectation values of various operators in the thermal vacuum given in Eq.(8). These expressions would be used to calculate thermal expectation value of the Hamiltonian to compute the thermodynamic potential. We define

$$\langle \Omega(\beta, \mu) | \tilde{\psi}_\alpha(\mathbf{k}) \tilde{\psi}_\beta(\mathbf{k}')^\dagger | \Omega(\beta, \mu) \rangle = \Lambda_{+\alpha\beta}(\mathbf{k}, \beta, \mu) \delta(\mathbf{k} - \mathbf{k}'), \quad (13)$$

and,

$$\langle \Omega(\beta, \mu) | \tilde{\psi}_\beta(\mathbf{k})^\dagger \tilde{\psi}_\alpha(\mathbf{k}') | \Omega(\beta, \mu) \rangle = \Lambda_{-\alpha\beta}(\mathbf{k}, \beta, \mu) \delta(\mathbf{k} - \mathbf{k}'), \quad (14)$$

where,

$$\Lambda_+(\mathbf{k}, \beta, \mu) = \frac{1}{2} \left(1 + F_1(\mathbf{k}) - F(\mathbf{k}) + (\gamma^0 \sin 2h(\mathbf{k}) + \boldsymbol{\alpha} \cdot \hat{\mathbf{k}} \cos 2h(\mathbf{k})) (1 - F(\mathbf{k}) - F_1(\mathbf{k})) \right), \quad (15)$$

and,

$$\Lambda_-(\mathbf{k}, \beta, \mu) = \frac{1}{2} \left(1 + F(\mathbf{k}) - F_1(\mathbf{k}) - (\gamma^0 \sin 2h(\mathbf{k}) + \boldsymbol{\alpha} \cdot \hat{\mathbf{k}} \cos 2h(\mathbf{k})) (1 - F(\mathbf{k}) - F_1(\mathbf{k})) \right). \quad (16)$$

Here, the effect of diquark condensate and the temperature and/or density dependence is encoded in the function $F(\mathbf{k})$ and $F_1(\mathbf{k})$ given as

$$F(\mathbf{k}) = \sin^2 f(\mathbf{k}) + \cos 2f(\mathbf{k}) \sin^2 \theta_-(\mathbf{k}, \beta, \mu), \quad (17)$$

and,

$$F_1(\mathbf{k}) = \sin^2 f_1(\mathbf{k}) + \cos 2f_1(\mathbf{k}) \sin^2 \theta_+(\mathbf{k}, \beta, \mu). \quad (18)$$

Clearly, at zero temperature and zero density the functions F and F_1 vanish and the projection operators reduce to the forms considered earlier [10],

$$\Lambda_\pm(\vec{k}, \beta) = \frac{1}{2} \left[1 \pm (\gamma^0 \sin 2h(k) + \vec{\alpha} \cdot \hat{k} \cos 2h(k)) \right]. \quad (19)$$

Further, at zero density but finite temperature $\theta_- = \theta_+$ and projection operators reduce to [25],

$$\Lambda_\pm(\vec{k}, \beta) = \frac{1}{2} \left[1 \pm \cos 2\theta (\gamma^0 \sin 2h(k) + \vec{\alpha} \cdot \hat{k} \cos 2h(k)) \right]. \quad (20)$$

We also have

$$\begin{aligned} \langle \Omega(\beta, \mu) | \psi_\alpha^{ia}(\vec{x}) \psi_\gamma^{jb} | \Omega(\beta, \mu) \rangle &= \frac{\epsilon^{ij} \epsilon^{3ab}}{(2\pi)^3} \int e^{i\mathbf{k} \cdot \mathbf{x}} \mathcal{P}_{+\gamma\alpha}(\mathbf{k}, \beta, \mu) d\mathbf{k}, \\ \langle \Omega(\beta, \mu) | \psi_\alpha^{ia\dagger}(\vec{x}) \psi_\gamma^{jb\dagger} | \Omega(\beta, \mu) \rangle &= \frac{\epsilon^{ij} \epsilon^{3ab}}{(2\pi)^3} \int e^{i\mathbf{k} \cdot \mathbf{x}} \mathcal{P}_{-\alpha\gamma}(\mathbf{k}, \beta, \mu) d\mathbf{k}, \end{aligned} \quad (21)$$

where,

$$\mathcal{P}_+(\mathbf{k}, \beta, \mu) = \frac{1}{4} \left[S(\mathbf{k}) + \left(\gamma^0 \sin 2h(\mathbf{k}) - \boldsymbol{\alpha} \cdot \hat{\mathbf{k}} \cos 2h(\mathbf{k}) \right) A(\mathbf{k}) \right] \gamma_5 C, \quad (22)$$

and,

$$\mathcal{P}_-(\mathbf{k}, \beta, \mu) = \frac{C\gamma_5}{4} \left[(S(\mathbf{k}) + \left(\gamma^0 \sin 2h(\mathbf{k}) - \boldsymbol{\alpha} \cdot \hat{\mathbf{k}} \cos 2h(\mathbf{k}) \right) A(\mathbf{k})) \right]. \quad (23)$$

Here, $C = i\gamma^2\gamma^0$ is the charge conjugation matrix (we use the notation of Bjorken and Drell) and the functions $S(\mathbf{k})$ and $A(\mathbf{k})$ are given as,

$$S(\mathbf{k}) = \sin 2f(\mathbf{k}) \cos 2\theta_-(\mathbf{k}, \beta, \mu) + \sin 2f_1(\mathbf{k}) \cos 2\theta_+(\mathbf{k}, \beta, \mu), \quad (24a)$$

and,

$$A(\mathbf{k}) = \sin 2f(\mathbf{k}) \cos 2\theta_-(\mathbf{k}, \beta, \mu) - \sin 2f_1(\mathbf{k}) \cos 2\theta_+(\mathbf{k}, \beta, \mu), \quad (24b)$$

Using Eq. (14) we have for the kinetic energy part

$$T \equiv \langle \Omega, \beta, \mu | \psi^\dagger (-i\boldsymbol{\alpha} \cdot \boldsymbol{\nabla}) \psi | \Omega \beta \mu \rangle = \frac{\gamma}{(2\pi)^3} \int d\mathbf{k} \cos 2h(\mathbf{k}) (1 - F - F_1), \quad (25)$$

where, the degeneracy factor $\gamma = 12$ corresponding to spin(2), color(3) and flavor(2) degrees of freedom. T in Eq.(25) above, however, includes the contribution of the perturbative zero point energy corresponding to $h(\mathbf{k}) = 0 = f(\mathbf{k}) = f_1(\mathbf{k})$. Subtracting this out we have the contribution from the kinetic energy

$$\mathcal{T} = T - \langle \hat{T} \rangle|_{h=f=f_1=\theta_{\pm}=0} = \frac{\gamma}{(2\pi)^3} \int |\mathbf{k}| [2 \sin^2 h(\mathbf{k}) + \cos 2h(\mathbf{k})(F + F_1)]. \quad (26)$$

Similarly the contribution from the interaction term in Eq.(12) after subtracting out the zero point perturbative energy turns out to be

$$\mathcal{V} \equiv \langle \Omega, \beta, \mu | \frac{g^2}{2} J_\mu^a J^{\mu a} | \Omega \beta \mu \rangle = V_1 + V_2 \quad (27)$$

where, the contribution V_1 arises from using Eq.s (13), (14) and is given as

$$V_1 = \frac{g^2}{2} N_f \frac{(N_c^2 - 1)}{2} 2(I_1^2 - 2I_2^2) = 8g^2(I_1^2 - 2I_2^2) \quad (28)$$

with,

$$I_1 = \frac{1}{(2\pi)^3} \int d\mathbf{k} (F - F_1) \quad (29)$$

and

$$I_2 = \frac{1}{(2\pi)^3} \int d\mathbf{k} (1 - F - F_1) \sin 2h(\mathbf{k}). \quad (30)$$

The term V_2 arises from using Eq.(22) and (23) and we have

$$V_2 = \frac{2g^2}{3} (-2I_3^2 + I_4^2), \quad (31)$$

where

$$I_3 = \frac{1}{(2\pi)^3} \int d\mathbf{k} S(\mathbf{k}) \quad (32)$$

and

$$I_4 = \frac{1}{(2\pi)^3} \int d\mathbf{k} A(\mathbf{k}) \sin 2h(\mathbf{k}). \quad (33)$$

Then the free energy density is

$$\mathcal{F} = \epsilon - \mu N = \mathcal{T} + \mathcal{V} - \mu N \quad (34)$$

where, μ is the chemical potential and N is quark number density. Further,

$$N = \langle \psi^\dagger \psi \rangle = \frac{\gamma}{(2\pi)^3} \int d\mathbf{k} (F - F_1) = \gamma I_1. \quad (35)$$

Finally, for the entropy density we have [17]

$$s = -\frac{\gamma}{(2\pi)^3} \int d\mathbf{k} (\sin^2 \theta_- \ln \sin^2 \theta_- + \cos^2 \theta_- \ln \cos^2 \theta_- + \sin^2 \theta_+ \ln \sin^2 \theta_+ + \cos^2 \theta_+ \ln \cos^2 \theta_+) \quad (36)$$

and the thermodynamic potential which is negative of pressure is given by [26]

$$\Omega = -\mathcal{P} = \epsilon - \mu N - \frac{1}{\beta} s \quad (37)$$

Now if we minimise the thermodynamic potential Ω with respect to $h(\mathbf{k})$, we get

$$\tan 2h(\mathbf{k}) = \frac{8g^2 I_2}{3|\mathbf{k}|} \equiv \frac{M}{|\mathbf{k}|}. \quad (38)$$

where, $M = 8g^2 I_2/3$. Substituting this back in Eq.(30) we have the mass gap equation

$$M = \frac{8g^2 I_2}{3} = \frac{8g^2}{3} \frac{1}{(2\pi)^3} \int \frac{M}{\sqrt{\mathbf{k}^2 + M^2}} (1 - F - F_1) d\mathbf{k}. \quad (39)$$

Clearly, the above includes the effect of diquark condensates as well as temperature and density through the functions F and F_1 given in Eq.s (17) and (18) respectively. The zero temperature and density limit is given by setting $F = 0 = F_1$ which has the same structure as in NJL model [7,15,10].

Next, minimising the thermodynamic potential Ω with respect to f and f_1 yields

$$\tan 2f(\mathbf{k}) = \frac{2g^2}{9} \frac{(2I_3 - I_4 \sin 2h)}{\sqrt{\mathbf{k}^2 + M^2} - \left(\mu - \frac{4g^2}{3} I_1\right)} \quad (40)$$

and,

$$\tan 2f_1(\mathbf{k}) = \frac{2g^2}{9} \frac{(2I_3 + I_4 \sin 2h)}{\sqrt{\mathbf{k}^2 + M^2} + \left(\mu - \frac{4g^2}{3} I_1\right)}. \quad (41)$$

We might further simplify equations (40) and (41) by noting from Eq.s (32), (33), (24b) and (24a) that the integral I_4 is small compared to I_3 , as the integrand in the former is a difference of two positive quantities whereas the latter is a sum of these two quantities. In addition, the integrand in I_4 is suppressed by the quark antiquark condensate function $\sin 2h(\mathbf{k})$ which is not the case in I_3 . Finally, this apart, in Eq.s (40) and (41) the numerical coefficient in the second term of the numerator is small compared to that in the first term. Thus, we can approximate

$$\tan 2f(\mathbf{k}) = \frac{\Delta}{E - \nu} \quad (42)$$

$$\tan 2f_1(\mathbf{k}) = \frac{\Delta}{E + \nu}, \quad (43)$$

where, the superconducting gap $\Delta = (4g^2/9)I_3$, $E = \sqrt{\mathbf{k}^2 + M^2}$ and $\nu = \mu - 4g^2/3I_1$ is the chemical potential in presence of interaction [12]. From the definition of superconducting gap and Eq.(32) we have the superconducting gap equation given by

$$\Delta = \frac{4g^2}{9} I_3 = \frac{4g^2}{9(2\pi)^3} \int d\mathbf{k} \left(\frac{\Delta}{\sqrt{\Delta^2 + (E - \nu)^2}} \cos 2\theta_-(\mathbf{k}, \beta, \mu) + \frac{\Delta}{\sqrt{\Delta^2 + (E + \nu)^2}} \cos 2\theta_+(\mathbf{k}, \beta, \mu) \right) \quad (44)$$

Finally, minimisation of the thermodynamic potential with respect to the thermal functions $\theta_{\pm}(\mathbf{k}, \beta, \mu)$ gives

$$\sin^2 \theta_- = \frac{1}{\exp(\beta\omega_-) + 1} \quad (45)$$

and

$$\sin^2 \theta_+ = \frac{1}{\exp(\beta\omega_+) + 1} \quad (46)$$

where, $\omega_{\pm} = \sqrt{\Delta^2 + \xi_{\pm}^2}$ and $\xi_{\pm} = (E \pm \nu)$. Therefore, with all the ansatz functions *determined* from the minimisation of the thermodynamic potential $\Omega(\beta, \mu)$, the mass gap equation (39) and superconducting gap equations are given respectively as

$$\frac{4g^2}{3} \frac{1}{(2\pi)^3} \int d\mathbf{k} \frac{1}{\sqrt{\mathbf{k}^2 + M^2}} \left(\frac{\xi_-}{\omega_-} \tanh\left(\frac{\beta\omega_-}{2}\right) + \frac{\xi_+}{\omega_+} \tanh\left(\frac{\beta\omega_+}{2}\right) \right) = 1 \quad (47)$$

$$\frac{4g^2}{9} \frac{1}{(2\pi)^3} \int d\mathbf{k} \left(\frac{\tanh(\frac{\beta\omega_-}{2})}{\omega_-} + \frac{\tanh(\frac{\beta\omega_+}{2})}{\omega_+} \right) = 1 \quad (48)$$

Equation (47) is the generalisation of the mass gap equation considered at zero temperature and density of Ref. [7,10] to include the effect of finite temperature and density [15] *alongwith* the effect of diquark condensates. Similarly, Eq.(48) is the relativistic generalisation of the BCS gap equation [15] in the presence of a dynamically generated mass gap through a quark antiquark condensate structure for the vacuum. These are the main new features of the present work.

IV. SOLUTION OF THE GAP EQUATIONS AND RESULTS

Before trying to solve the coupled gap equations (47) and (48) we discuss the solutions in the following two different limiting cases, so that we make connection with earlier studies [12,15].

- Case-I : Only quark antiquark condensate i.e. $h(\mathbf{k}) \neq 0$; $f(\mathbf{k}) = 0 = f_1(\mathbf{k})$
In this limit $\Delta = 0$ and the gap equation (47) reduces to

$$M = \frac{8g^2}{3} \frac{1}{(2\pi)^3} \int \frac{M}{\sqrt{\mathbf{k}^2 + M^2}} (1 - n_+ - n_-) d\mathbf{k} \quad (49)$$

where,

$$n_{\pm} = \frac{1}{\exp(\beta(E(\mathbf{k}) \pm \nu)) + 1}$$

This is the same equation as obtained in Ref. [7,28,29] except for numerical factors before the integrand. This is due to the difference in the Lorentz structure of the four fermion interaction term. In Ref. [7] the interaction term is $(\bar{\psi}\psi)^2 + ((\bar{\psi}\gamma_5\tau\psi)^2)$ that can originate from a Fierz transformation of the $J_{\mu}^a J^{\mu a}$ interaction as considered here. In Ref. [29] only $J_0^a J^{0a}$ term was included. We might however mention here that keeping $J_0 J_0$ term only will make the pressure negative at high densities even when the condensate vanishes. At zero temperature the mass gap is given by the solution of the equation

$$\frac{4g^2}{3\pi^2} \int_{k_f}^{\Lambda} \frac{k^2 dk}{\sqrt{k^2 + M^2}} = 1 \quad (50)$$

where the fermi mometum k_f is defined through the (interacting) chemical potential ν as $k_f^2 + M^2 = \nu^2$. We also note that this gap equation is derived here by minimising the thermodynamic potential over a variational ansatz and not through a mean field approximation [28] or a Hartree Fock calculation [7]. The critical fermi momentum is given by the density where $M = 0$ and is given at zero temperature by,

$$k_f^c = \Lambda \left(1 - \frac{3\pi^2}{2g^2\Lambda^2} \right)^{1/2} \quad (51)$$

and the corresponding quark number density is given by $n_0 = \gamma k_f^c{}^3 / 6\pi^2$. The variation of mass gap as a function of fermi momentum is shown in Fig. (1). We have chosen the value of the coupling $g^2 = 55.98 GeV^{-2}$ and $\Lambda = 0.67 GeV$ as typical values. In fact, they have been chosen so that the diquark condensate function vanishes at the same critical temperature as in Ref. [12,15].

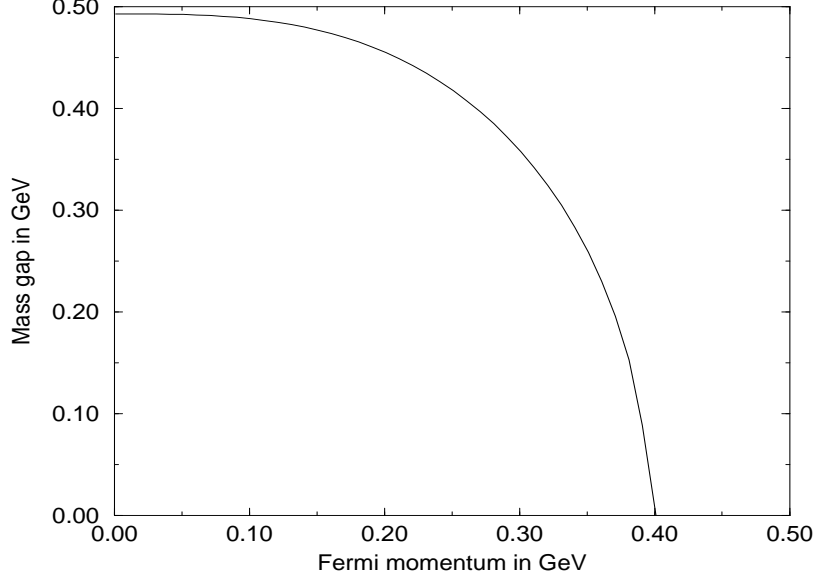


FIG. 1. *Mass gap vs fermi mometum. Critical fermi mometum turns out to be 0.39 GeV corresponding to a quark number density of 1.7 per fm^3 .*

With this choice of parameters, the dynamically generated quark mass at zero temperature and density becomes about 490 GeV which is rather high compared to the standard value of around 300 MeV. With a lower value of $g^2\Lambda^2$ the same could be made smaller. The critical density in this model turns out to be about $1.7/\text{fm}^3$ corresponding to a value of the fermi momentum k_f^c of 0.4GeV . In Fig.2 we have plotted the pressure as a function of fermi momentum. Here we have added the bag constant ϵ_0 which is the energy density at zero quark number density at zero temperature [8]. This turns out to be about $-(0.2\text{GeV})^4$. As observed earlier [12] the pressure has a cusp like structure and becomes negative at finite density. The portion of the curve that goes down with fermi momentum corresponds to a nontrivial mass gap solution and the portion that increases with density correponds to zero mass solution of the mass gap equation (47). As in Ref [15], and unlike Ref. [12] the effects of interactions do not disappear beyond the chiral symmetry restoration phase. This is due to the fact that there is no running coupling involved here and in fact, the pressure grows as n^2 or k_f^6 at high densities as may be expected from the interaction term V_1 involving $I_1^2 = N^2/\gamma^2$ given in Eq.(28). However, one has to keep in mind that to be consistent with the philosophy of high momentum cutoff Λ , the fermi momentum should be less than the cut off momentum. The negative pressure at intermediate densities can be understood in terms of mechanical instability and can have the interpretation that uniform nonzero density quark matter will break up into droplets of finite density in which chiral symmetry is restored surrounded by empty space with zero pressure and density. It is tempting to identify these droplets with nucleons within which the density is nonzero and $\langle\bar{q}q\rangle=0$ — a fact reminiscent of bag models. Nothing within the model however implies that the droplets have quark number three [12].

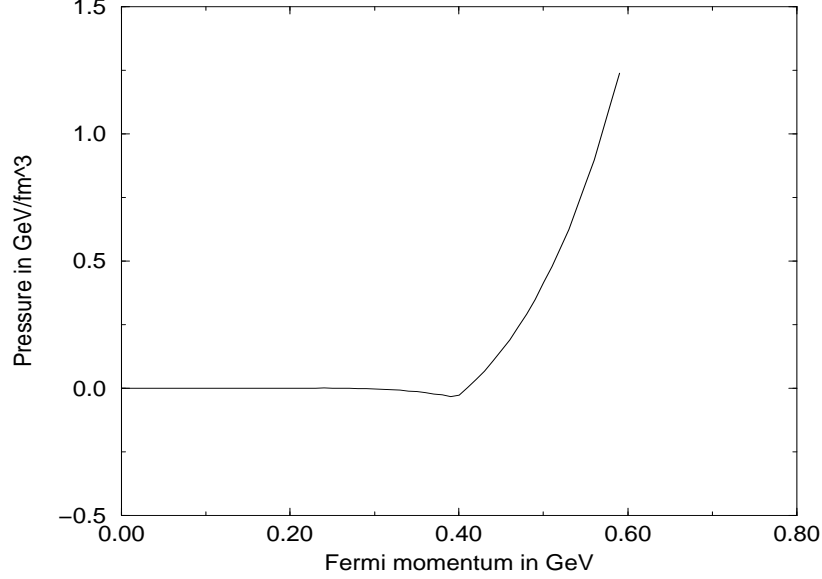


FIG. 2. Pressure as a function of fermi mometum. The decreasing part of the curve corresponds to $m \neq 0$ solution and the rising part of the curve corresponds to $m = 0$ solution of the mass gap equation (47)

- Case- II: No chiral condensate but only diquark condensate i.e. $h(\mathbf{k}) = 0$, $f(\mathbf{k}) \neq 0$, $f_1(\mathbf{k}) \neq 0$

In this case, the quark mass arising from chiral condensate is zero and the superconducting gap equation (48) reduces to

$$1 = \frac{2g^2}{9\pi^2} \int_0^\Lambda k^2 dk \left[\frac{1}{\omega_-} \tanh\left(\frac{\beta\omega_-}{2}\right) + \frac{1}{\omega_+} \tanh\left(\frac{\beta\omega_+}{2}\right) \right] \quad (52)$$

where, as before $\omega_\pm = \sqrt{\Delta^2 + \xi_\pm^2}$ but, with $\xi_\pm = |\mathbf{k}| \pm \nu$. This is the relativistic generalisation of BCS gap equation in superconductivity [23]. It has the same structure as in Ref [12] in the limit the form factor is replaced by a sharp cutoff as in Ref. [15] and apart from the numerical factor preceeding the integrand. Further, this can be rearranged to interpret separately contributions arising from particles, antiparticles and holes [12]. We have chosen the values of the coupling and the cutoff as in Ref. [15] so as to get the same critical temperature as in Ref. [12]. The gap equation at zero temperature is given as

$$1 = \frac{2g^2}{9\pi^2} \int_0^\Lambda k^2 dk \left[\frac{1}{\omega_-} + \frac{1}{\omega_+} \right] \quad (53)$$

The superconducting gap Δ is plotted in Fig 3. While obtaining the solution of the gap equation (53) we also insist that a nontrivial solution of the gap equation is acceptable only if the corresponding free energy is smaller than that with no gap. The gap increases with fermi momentum, has a maximum of about 90 MeV around fermi momentum 550 MeV, beyond which the effect of cutoff is felt and it vanishes at around $k_f = 600$ MeV.

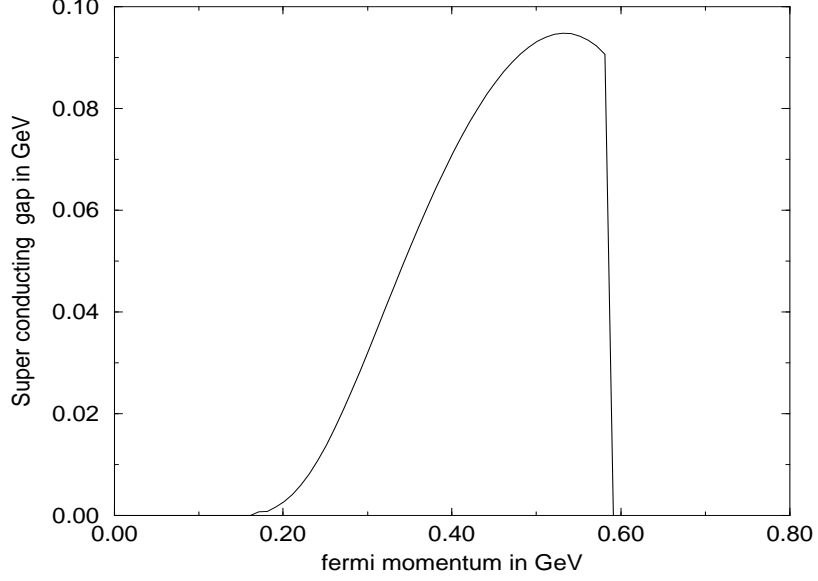


FIG. 3. *Superconducting gap vs fermi mometum.*

The resulting equation of state i.e. pressure as a function of fermi momentum is plotted in Fig.4. There is no unstable phase as discussed for chiral condensate case with negative pressure. Because of the interaction term, the equation of state does not go over to the free massless equation of state beyond the critical density. We have plotted the pressure in Fig.4 for fermi momentum upto 600 MeV noting that the cutoff here is about 650 MeV.

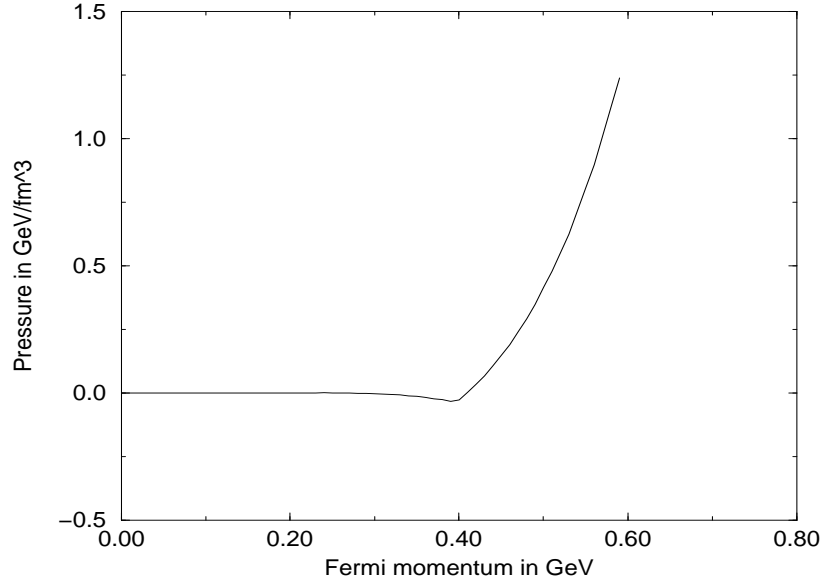


FIG. 4. *Pressure vs fermi mometum.*

- Case- III: $h(\mathbf{k}) \neq 0; f(\mathbf{k}) \neq 0$ and $f_1(\mathbf{k}) \neq 0$.

Here we solve the coupled gap equations (47) and (48) which at zero temperature but finite density reduce to

$$\frac{2g^2}{3\pi^2} \int dk \frac{k^2}{E} \left(\frac{\xi_-}{\omega_-} + \frac{\xi_+}{\omega_+} \right) = 1 \quad (54)$$

$$\frac{2g^2}{9\pi^2} \int dk k^2 \left(\frac{1}{\omega_-} + \frac{1}{\omega_+} \right) = 1 \quad (55)$$

where, $\omega_{\pm} = \sqrt{\Delta^2 + \xi_{\pm}^2}$; $\xi_{\pm} = E \pm \nu$ and $E = \sqrt{\mathbf{k}^2 + M^2}$. To solve the above equations numerically, we take ν as an input and obtain the values of mass gap M and the superconducting gap Δ so that both the equations are satisfied simultaneously. The chemical potential ν is related to the fermi momentum as $k_f = \sqrt{\nu^2 - M^2}$. The resulting mass gap and the superconducting gap are plotted in Fig. 5 and Fig 6 respectively. For the sake of comparison we have also plotted the mass gap without diquark condensate (case-I) in Fig 5, and, superconducting gap without chiral gap (case-II) in Fig. 6. As may be noted, the mass gap does not change very much through the inclusion of diquark condensates. The superconducting gap however starts at a lower threshold and varies slowly compared to the case of no mass gap. Both the curves however merge at the chiral restoration point.

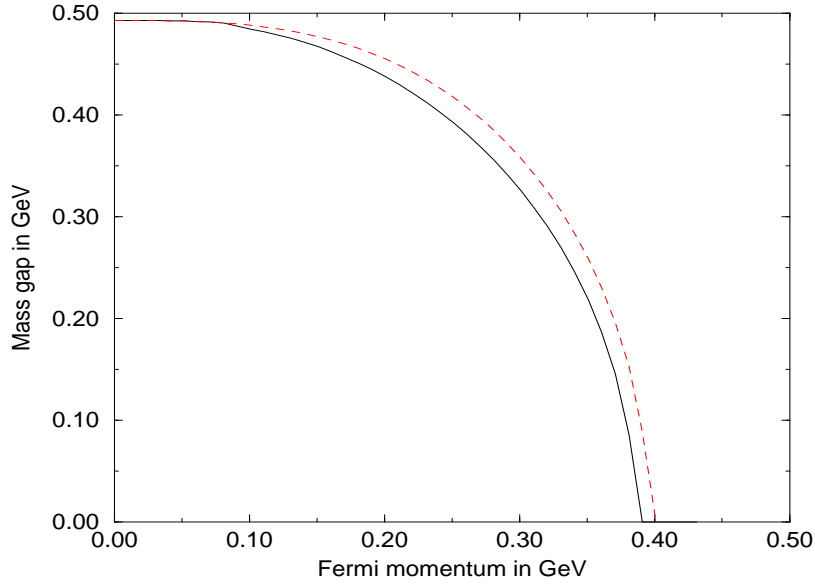


FIG. 5. Mass gap M as a function of fermi mometum. The dashed line correspond to no diquark condensates. The solid line corresponds to both diquark and quark antiquark condensates.

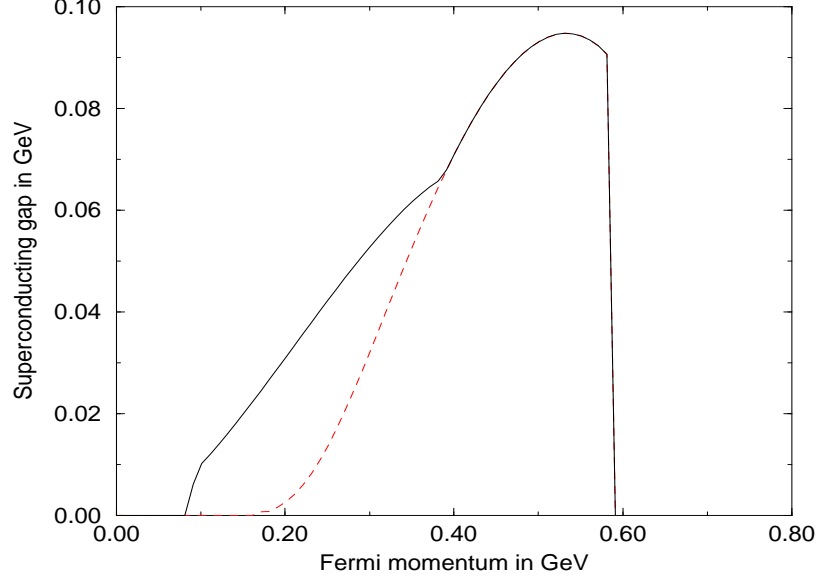


FIG. 6. Superconducting gap Δ as a function of fermi mometum . The solid line corresponds to both diquark and quark antiquark condensates. The dashed line corresponds to only diquark condensates.

We have also plotted the equation of state , pressure as a function of fermi momentum in Fig.7. The equation of state does not change very much compared to the case with only quark antiquark condensates.

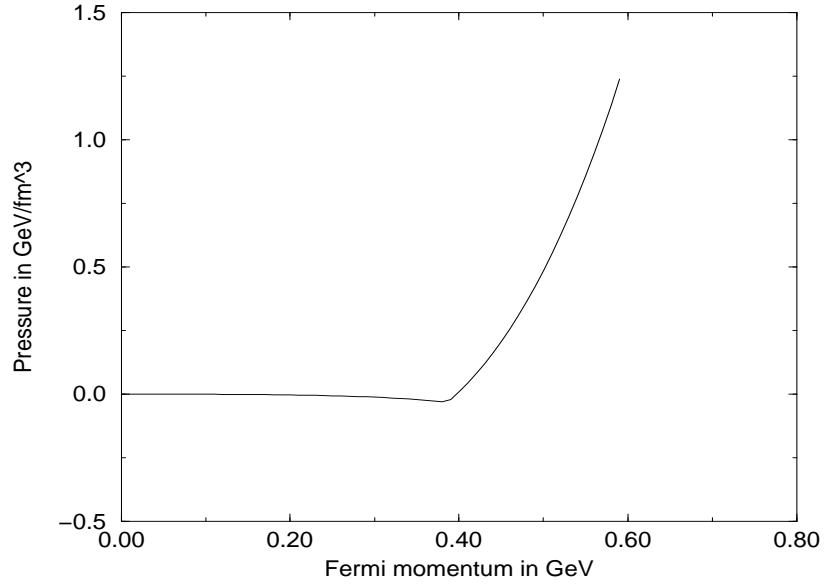


FIG. 7. Pressure as a function of fermi momentum .

This should be expected as the effect of diquark condensate is small in the region where chiral condensate is nonvanishing. As may be evident from Fig.[6] there is a region from $k_f \simeq 0.1$ fm till $k_f \simeq 0.4$ fm where simultaneous existence of both types of condensates is possible. However, in this region the pressure becomes

negative. As in case I, this will correspond to mechanical instability. The finite density matter will break into droplets of finite density in which chiral symmetry is restored and the matter is in a superconducting phase surrounded by empty space with zero pressure and density. Below $k_f = 0.1$ fm the phase with only quark antiquark condensates and for $k_f > 0.4$ fm the phase with diquark condensates is thermodynamically feasible. However, one should not extrapolate to fermi momenta higher than the cutoff momentum of the model to be consistent with the philosophy of high momentum cutoff.

A. The phase diagram

To discuss the phase diagram we have solved the two gap equations Eq.(47) and Eq. (48) at finite temperature and density to calculate different thermodynamic quantities. The result of such a calculation for the mass gap is shown in Fig.(8). Similarly the superconducting gap at different temperatures is shown in Fig.(9).

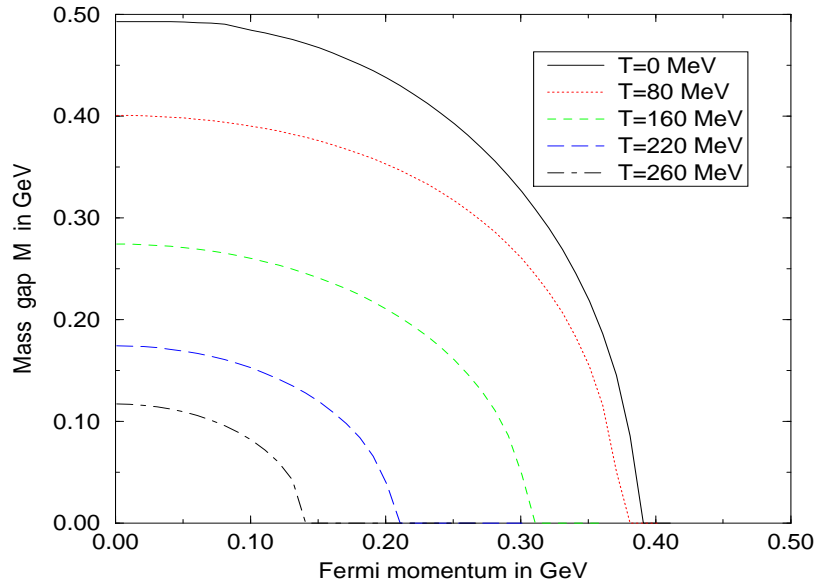


FIG. 8. Mass gap at different temperatures as a function of fermi momentum.

The superconducting gap decreases with temperature and vanishes at around 55 MeV. Similarly the mass gap also decreases with temperature and vanishes at about 270 MeV at zero density. The superconducting transition is a second order phase transition. The chiral phase transition is first order at zero density but is second order at high temperature. The pressure at different temperatures is shown in Fig.10 as a function of $(n/n_0)^{1/3}$, where n is number density and $n_0 = (2/\pi^2)\nu_c^3$ is the critical number density at zero temperature. The cusp in the pressure density curve, indicating a first order phase transition, vanishes at about 84 MeV. At temperatures beyond that the pressure increases monotonically with density.

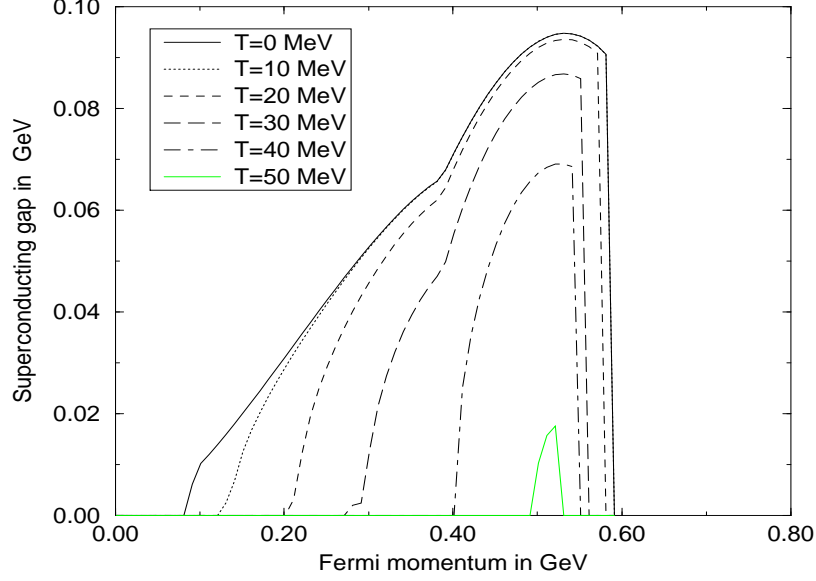


FIG. 9. Superconducting gap at different temperatures as a function of fermi momentum.

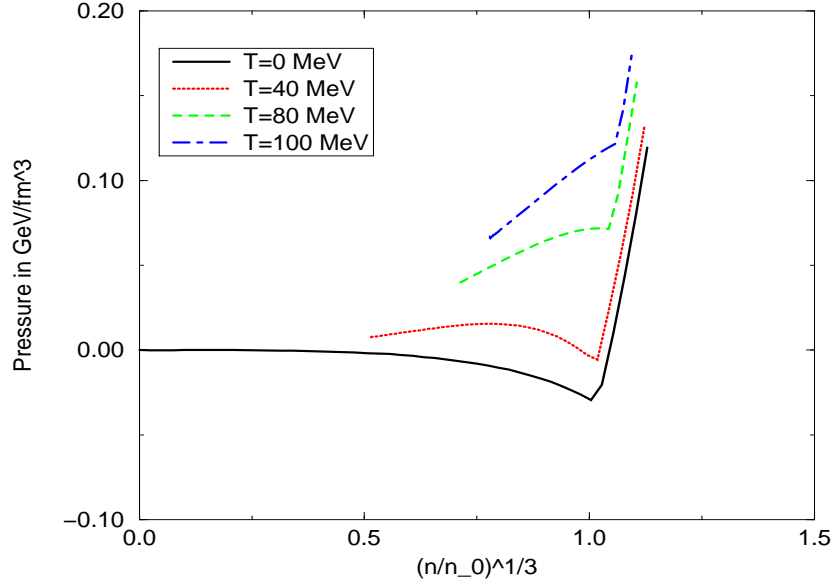


FIG. 10. Pressure as a function of density at different temperatures. The tricritical point turns out to be about 84 MeV.

To discuss the critical line for the chiral transition in the number density and temperature plane we need to solve the gap equation (47) with mass gap equated to zero i.e. the critical line satisfies the equation

$$\frac{4g^2}{3\pi^2} \int_0^\Lambda dk k \left(1 - \frac{1}{\exp(\beta(k-\nu)) + 1} - \frac{1}{\exp(\beta(k+\nu)) + 1} \right) = 1 \quad (56)$$

As the distribution functions are rapidly decreasing functions of momentum we may approximate the upper limit $\Lambda \rightarrow \infty$. In that case Eq.(56) reduces to

$$\nu^2 + \tau^2 = \nu_c^2 \quad (57)$$

where, $\tau = \pi T/\sqrt{3}$ and $\nu_c \equiv k_f^c = \Lambda(1 - 3\pi^2/(2g^2\Lambda^2))$, the critical chemical potential or fermi momentum at zero temperature calculated earlier in Eq.(51). It may be useful to write down this relation in terms of number densities rather than the chemical potential using the relation

$$n = \frac{6}{\pi^2} \int_0^\Lambda dk k^2 \left(\frac{1}{\exp(\beta(k - \nu)) + 1} - \frac{1}{\exp(\beta(k + \nu)) + 1} \right) \approx \frac{2}{\pi^2} \nu(\nu^2 + \pi^2 T^2) \quad (58)$$

where, we again take infinity as the upper limit in the momentum integration as was done in Eq.(56). This leads to the equation for the critical line in the number density plane as

$$n/n_0 = \left(1 - \left(\frac{\tau}{\nu_c} \right)^2 \right)^{1/2} \left(1 + 2 \left(\frac{\tau}{\nu_c} \right)^2 \right) \quad (59)$$

where, $n_0 = (2/\pi^2)\nu_c^3$ is the critical density at zero temperature. This approximate solution is shown by the dotted line in Fig.11. The numerical solution for the critical line with the finite cutoff for the momentum is shown by the solid curve in the same figure. As the chiral phase transition is a first order phase transition at zero temperature and is second order at high temperature there will be a tricritical point for the chiral phase transition below which there will be a mixed phase. This mixed phase here will correspond to the phase with droplets of finite density quark matter in the superconducting but chiral symmetric phase surrounded by empty space with $n = 0, P = 0, \Delta = 0$ and chiral symmetry broken phase. This can be obtained by a Maxwell construction to exclude the part of the phase diagram where pressure decreases with density. This is shown as the dashed curve in Fig.11. The tricritical point in this model turns out to be 84 MeV [15,16].

We have also shown in Fig.11 the critical line for the color superconducting phase by the dot-dashed line. The decreasing part of this line is due to the fact that we have taken a cut off in the momentum and at high enough density the superconducting gap vanishes as shown in Fig. 9.

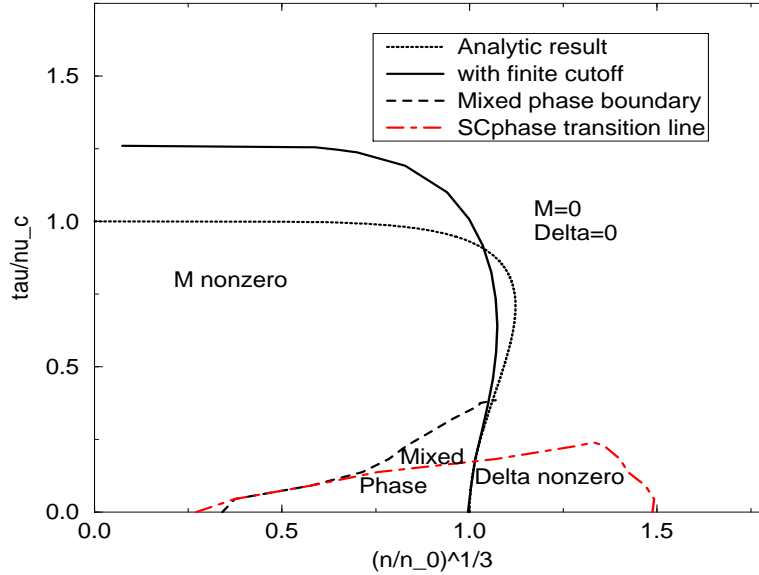


FIG. 11. Phase diagram in density temperature plane

A detailed quantitative comparison of our results with those in Ref. [16] is not very meaningful since our model is a simple, schematic one. However, it is very reassuring that the structure of the phase diagram is very similar to the one obtained by Berges and Rajagopal [16].

V. SUMMARY

We have analysed in a current current point interaction model the structure of vacuum with quark antiquark as well as diquark pairs. The methodology used is a variational one with an explicit construct of the trial state. The present work is not based on a mean field approximation [28]. Because of the point interaction structure we could solve for the gap functions explicitly. If we had taken the interaction term with a potential the gap equation would become an integral equation. It will be interesting to include a realistic effective potential and solve for the gap equation. There appears to be a region depending upon the coupling where both chiral condensates as well as diquark condensates are thermodynamically feasible. Presence of diquark condensate does not modify the dynamical mass of the quarks. The dynamical mass however affects the threshold for superconducting gap. The equation of state does not differ very much with inclusion of diquark condensates. We also obtain the complete phase diagram of the system in overall agreement with that of Ref. [16]. Finally, our results suggests that our simple model contains the essential physics of the system.

ACKNOWLEDGMENTS

HM would like to thank Amruta Mishra for numerous discussions.

-
- [1] E.V. Shuryak, *The QCD vacuum, hadrons and the superdense matter* (World Scientific, Singapore, 1988).
 - [2] M.A. Shifman, A.I. Vainshtein and V.I. Zakharov, Nucl.Phys. B147, 385, 448 and 519(1979).
 - [3] Y. Nambu, Phys. Rev. Lett. **4**, 380 (1960); A. Amer, A. Le Yaouanc, L. Oliver, O. Pene and J.C. Raynal, Phys. Rev. Lett.**50**, 87 (1983); *ibid*, Phys. Rev.**D28**, 1530 (1983); M.G. Mitchard, A.C. Davis and A.J. Macfarlane, Nucl. Phys. **B325**, 470 (1989); B. Haeri and M.B. Haeri, Phys. Rev.**D43**, 3732 (1991); V. Bernard, Phys. Rev.**D34**, 1601 (1986); S. Schram and W. Greiner, Int. J. Mod. Phys. **E1**, 73 (1992)
 - [4] J.R. Finger and J.E. Mandula, Nucl. Phys. **B199**, 168 (1982).
 - [5] S.L. Adler and A.C. Davis, Nucl. Phys.**B244**, 469 (1984) .
 - [6] R. Alkofer and P. A. Amundsen, Nucl. Phys.**B306**, 305 (1988)
 - [7] S.P. Klevensky, Rev. Mod. Phys.**64**, 649 (1992);
 - [8] S. Li, R.S. Bhalerao and R.K. Bhaduri, Int. J. Mod. Phys. **A6**, 501 (1991)
 - [9] A. Mishra, H. Mishra and S.P. Misra, Z. Phys. C 57, 241 (1993)
 - [10] H. Mishra and S.P. Misra, Phys. Rev. D 48, 5376 (1993)
 - [11] R. Alkofer, P. A. Amundsen and K. Langfeld, Z. Phys. C 42, 199(1989), A.C. Davis and A.M. Matheson, Nucl. Phys. B246, 203 (1984).
 - [12] M. Alford, K.Rajagopal, F. Wilczek, Phys. Lett. B422,247(1998); *ibid* Nucl. Phys. B537,443 (1999).
 - [13] R.Rapp, T.Schaefer, E. Shuryak and M. Velkovsky Phys. Rev. Lett. 81, 53(1998); *ibid*, hep-ph/9904353.
 - [14] D. Bailin and A. Love, Phys. Rep. 107 (1984) 325, D. Son, Phys. Rev. D59 (1999) 094019, T. Schaefer and F. Wilczek, Phys. Rev. D60 (1999) 114033, D. Rischke and R. Pisarski, Phys. Rev. D61 (2000) 051501, D. K. Hong, V. A. Miransky, I. A. Shovkovy, L.C. Wiewewardhana, Phys. Rev. D61 (2000) 056001.
 - [15] T.M. Schwartz, S.P. Klevansky, G. Papp, Phys. Rev. C (1999)
 - [16] J. Berges, K. Rajagopal, Nucl. Phys. B538, 215, (1999).
 - [17] H. Umezawa, H. Matsumoto and M. Tachiki *Thermofield dynamics and condensed states* (North Holland, Amsterdam, 1982) ; P.A. Henning, Phys. Rep.253, 235 (1995).
 - [18] S.P. Misra, Talk on ‘Phase transitions in quantum field theory’ in the Symposium on Statistical Mechanics and Quantum field theory, Calcutta, January, 1992, hep-ph/9212287
 - [19] A. Mishra and S.P. Misra, Z. Phys. C 58, 325 (1993)
 - [20] S.P. Misra, Phys. Rev. D18, 1661 (1978); *ibid* D18, 1673 (1978)
 - [21] A. Le Youanc, L. Oliver, S. Ono, O. Pene and J.C. Raynal, Phys. Rev. Lett. 54, 506 (1985)
 - [22] S.P. Misra, Indian J. Phys., **70A**, 355 (1996)
 - [23] A.L. Fetter and J.D. Walecka, *Quantum Theory of Many particle Systems* (McGraw-Hill, New York, 1971).
 - [24] Amruta Mishra and Hiranmaya Mishra, J. Phys. G23,143, (1997).
 - [25] V. Sheel, H. Mishra and J.C. Parikh, Phys. Rev D59,034501 (1999); *ibid* Prog. Theor. Phys. Suppl.,129,137, (1997).
 - [26] A. Mishra, H. Mishra, S.P. Misra and S.N. Nayak, Z. Phys. C 57, 233 (1993); A. Mishra, H. Mishra and S.P. Misra, Z. Phys. C 58, 405 (1993)

- [27] M. Le Bellac, *Thermal Field Theory*(Cambridge, Cambridge University Press, 1996).
- [28] M. Asakawa and K. Yazaki, Nucl. Phys. A504,668 (1989).
- [29] Aleksander Kocic, Phys. Rev. D33, 1785,(1986).